Engenharia Agrícola

ISSN: 1809-4430 (on-line)

www.engenhariaagricola.org.br

Technical Paper
Doi: http://dx.doi.org/10.1590/1809-4430-Eng.Agric.v42n6e20220049/2022

DESIGN AND EXPERIMENT OF A CLAMP-HOLDING PRECISION MAIZE-SEED-METERING DEVICE

Xuejun Zhang[1*], Jinpeng Cheng[1], Zenglu Shi[1], Yunhe Zhang[1], Meijing Wang[1]

[1*]Corresponding author. College of Mechanical and Electrical Engineering, Xinjiang Agricultural University/ Urumqi, China. E-mail: tuec@163.com | ORCID ID: http://orcid.org/0000-0002-4413-3302

KEYWORDS

agricultural machinery, seed-metering device, maize, experiment, precision.

ABSTRACT

To solve the current problems of poor seeding stability and complex maintenance of maize seed-metering devices, a clamp-holding precision maize-seed-metering device is designed. The structure and working principle of the seed-metering device are described, the optimum state of maize seed clamping is analyzed, and the range of each working area of the seed-metering device is determined. The profile and structural parameters of the limit guide plate are designed by analyzing the laws of motion of the seed-picking block. A mechanical model of maize seeds under the critical state in each working area of the seed-metering device is established. The influence of the seed-metering device's rotational speed and the clamping force of the seed-picking block on the seeding performance are analyzed. A physical prototype of the seed-metering device was made for bench tests and field verification tests. The qualified, multiple seeding, and missed seeding rates of the designed seed-metering device were 94.21%, 3.52%, and 2.27%, respectively, meeting the agronomic requirements of maize sowing. The study provides theoretical guidance for designing and optimizing precision maize-seed-metering devices.

INTRODUCTION

Precision sowing technology is widely used in crop production because of its advantages of seed savings, yield improvement, and rational use of resources (Wang et al., 2022). The seed-metering device is a key component in this technology (Singh et al., 2020; Inderpal et al., 2020; Singh et al., 2021). Their efficiency and reliability play a decisive role in sowing quality and ensuring that agronomic production is carried out properly (Balappa et al., 2021; Zhang et al., 2021a). Currently, there are two main types of maize seed-metering devices: pneumatic and mechanical (Liao et al., 2020). The pneumatic seed-metering device still accounts for a relatively small proportion of field production due to its complex structure, high sealing requirements, and poor adaptability to field conditions (Li et al., 2020). Therefore the mechanical maize seed-metering devices are widely used in maize sowing operations (Astanakulov et al., 2021).

Depending on the working principle, mechanical maize seed-metering devices can be divided into scoop-wheel, finger-clamping, disc, and telescopic rod types (Yuan et al., 2018; Yang et al., 2016). Scholars worldwide have conducted much research on mechanical maize seed-metering devices in recent years (Wang et al., 2019a; Li et al., 2014). Wang et al. (2019b) designed a precision maize-seed-metering device by analyzing the seed-filling process and the variation law of seed-filling force. Geng et al. (2016) analyzed the force on seeds and designed a telescopic finger clip seed-metering device to improve the speed of sowing operations. Li et al. (2004) designed a tilting disc-type precision seed-metering device for maize based on the analysis of seed scoop characteristics and seed dispersal performance. Pareek et al. (2021) used the integrated ANN-PSO method to optimize the operating parameters of the tilting disc planter and obtained the optimum forward speed, tilting angle of the row of seeding plates and seed height. Although the above mechanical precision maize-seed-metering devices'

[1] College of Mechanical and Electrical Engineering, Xinjiang Agricultural University/Urumqi, China.

Area Editor: Francisco Scinocca
Received in: 4-1-2022
Accepted in: 10-25-2022

qualified seeding rate has met sowing needs, there are still problems such as lack of seeding stability, high structural integrity that precludes easy disassembly, and field operation and maintenance difficulties.In view of the above problems, this paper designs a new type of maize precision seed-metering device, which can effectively improve the seeding qualification rate and ensure the operation quality, and verifies the operation of the designed mechanism through experiments.

STRUCTURE AND WORKING PRINCIPLE

Main structure

As shown in Figure 1, the clamp-holding precision maize-seed-metering device consists of a seed inlet, fixed disc, seed spacer steel ring, pressure disc, core disc, limit guide plate, seed pick-up module assembly, moving disc, and shaft.

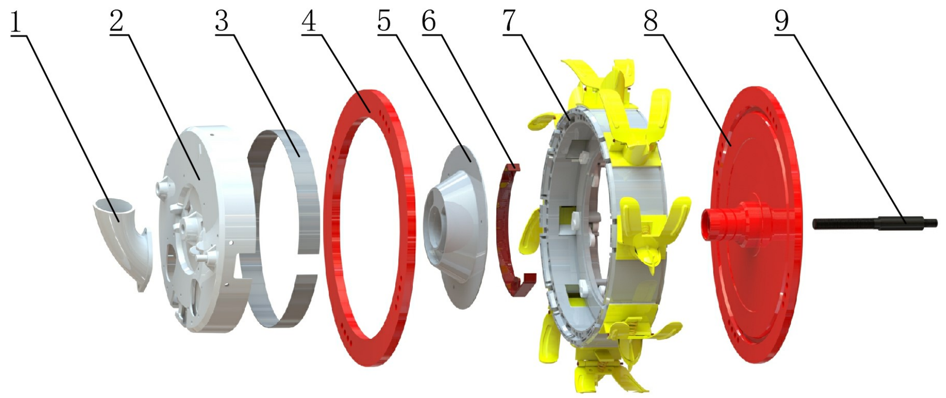

1. seed inlet 2. fixed disc 3. seed spacer steel ring 4. pressure disc 5. core disc 6. limit guide plate 7. seed pick-up module assembly 8. moving disc 9. shaft

(a) Schematic diagram of the seed-metering device's structure

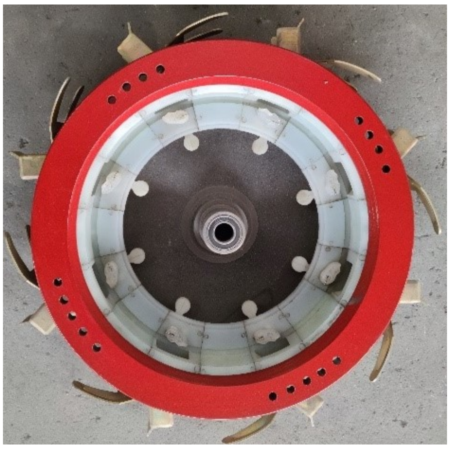

(b) Physical view of the seed-metering device

FIGURE 1. Clamp-holding precision maize-seed-metering device.

The seed inlet and the seed spacer steel ring are distributed on both sides of the inner and outer sides of the fixed disc. The limit guide plate is bolted to the inner side of the core disc. The eight individual seed pick-up modules are fitted together employing slots to form a seed pick-up module assembly, which is fixed axially on both sides using a pressure disc and moving disc. Each part is connected and fixed with shafts and bolts to form the whole seed-metering device. To reduce the impact on the maize seed cluster during the movement of the seed pick-up module, the seed-metering device is divided into a seed transport room and a seed control room using the core disc, the structure of which is shown in Figure 2. In the control room, the inflection arm and the limit guide plate are in constant contact and separation, thus controlling the seed-picking block in the seed transport chamber to form different clamp-holding angles with the seed spacer steel ring to complete the movement of seed filling and seed dropping.

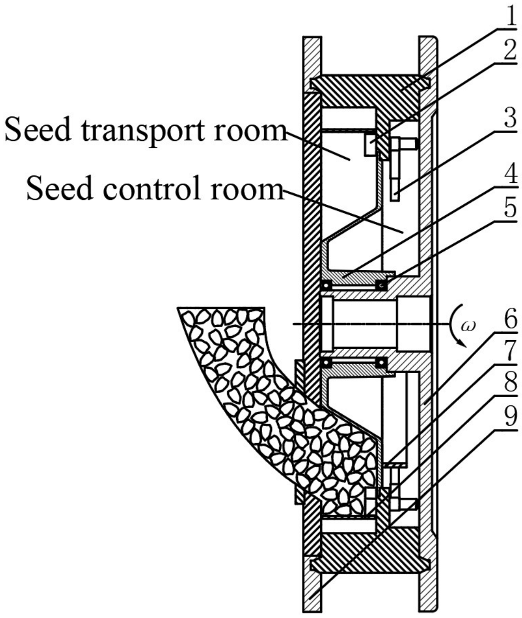

1. pick-up module 2. seed-picking block 3. inflection arm 4. core disc 5. bearing 6. moving disc 7. limit guide plate 8. seed spacer steel ring 9. pressure disc

FIGURE 2. Cutaway view of the seed-metering device.

The seed extraction mechanism is one of the core components of the seed-metering device. Its design determines the device's operational performance. As shown in Figure 3, the seed extraction mechanism is mainly composed of a torsion spring, bushing, inflection arm, bearing, seed-picking block, etc., where the seed-picking block and inflection arms are mounted on a common axis for synchronous rotation to meet the opening and closing requirements of different working areas.

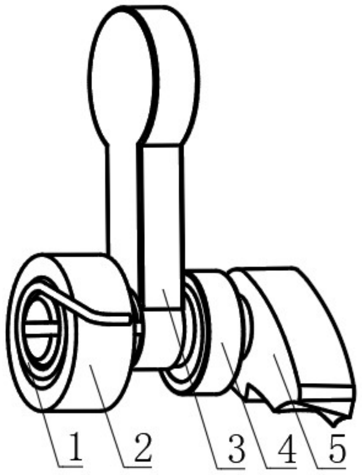

1. torsion spring 2. bushing 3. inflection arm 4. bearing 5. seed-picking block

FIGURE 3. Seed extraction mechanism.

Working principle

As shown in Figure 4, the working process of the seed-metering device is divided into four processes: seed filling, seed holding, seed cleaning, and seed dropping, of which the seed-dropping process is divided into the first seed-dropping process and the second seed-dropping process.

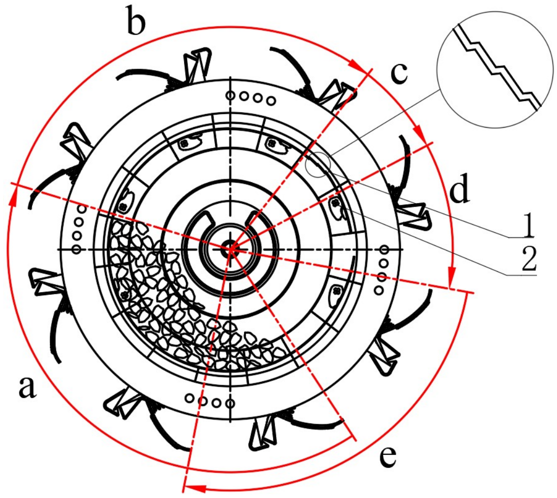

(a) seed-filling area, (b) seed-holding area, (c) seed-clearing area, (d) first seed-dropping area, and (e) second seed-dropping area

(1) Working process of the seed-metering device

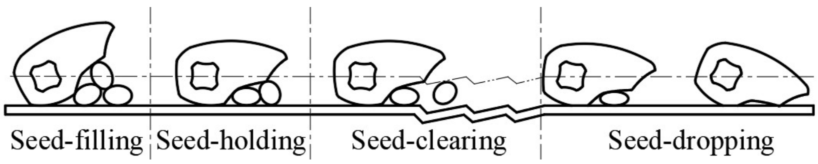

(2) Work process unfolding diagram

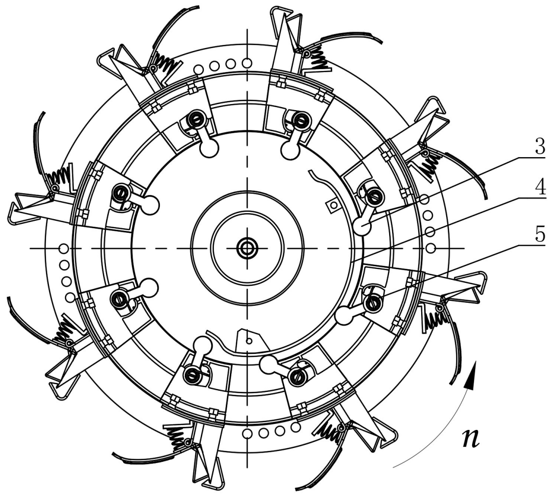

(3) Rear-view schematic

1. seed-clearing structure 2. seed-picking block 3. inflection arm 4. limit guide plate 5. torsion spring.

FIGURE 4. Working schematic diagram

During operation, the maize kernels enter the seed transport room of the seed-metering device through the seed inlet and form a cluster of kernels in the seed-filling area. The seed extraction mechanism follows the seed pick-up module in a rotary motion under a power drive, while the core disc is at rest under the limiting effect of the fixed disc. When the inflection arm on the seed extraction mechanism makes contact with the limit guide plate fixed on the core tray, the seed-picking block opens and forms a seed-filling space with the seed spacer steel ring. The maize seed enter the seed-filling space by gravity, centrifugal force, and the interaction between the seeds. After the end of contact movement between the inflection arm and the limit guide plate, the seed-picking block continues to push the seeds by the spring force of the torsion spring. When moving into the seed-clearing area, the excess clamped seeds fall back into the seed-filling area by gravity and the seed-clearing structure. The remaining clamped maize seeds continue to move to the first seed-dropping area. The seed storage chamber is entered under the action of gravity, centrifugal force, and the spring force of the torsion spring, at which point the seed-picking block loses support from the seed, the torsion spring springs back, the seed-picking block comes into contact with the seed spacer steel ring and the seed-filling space is closed, thus completing the first seed-dropping process. The seed entering the seed storage chamber enter the second seed-dropping area with the rotary movement of the seed pick-up module and complete the second seed-dropping process with the opening of the duckbill under gravity. The range of the seed-filling area is set at 130°, the seed-holding area at 110°, the seed-clearing area at 30°, the first seed-dropping area at 40°, and the second seed-dropping area at 90°, taking into account the position of the seed cluster in the seed-metering device and the horizontal height of the seed inlet.

Design and analysis of crucial components

Geometric parameters of maize seeds

The geometrical parameters of maize seeds are an essential basis for designing the critical structures of the seed-metering device (Liu et al., 2010). The geometrical dimensions of the different seeds provide an essential reference for the design of the seed-picking block. In this paper, Denghai 8883, Xingyu 33, and Liaozuo 1, widely grown in northern China, are selected for measurement, as shown in Figure 5. They are measured for length, width, and thickness, and the results are shown in Figure 6. The size of maize kernels varies considerably both between different varieties and between the same variety. It is therefore necessary to design a seed-metering device that can be applied to all sizes of maize seeds.

(a) Denghai 8883 (b) Xingyu 33 (c) Liaozuo 1

FIGURE 5. Classification of maize kernels.

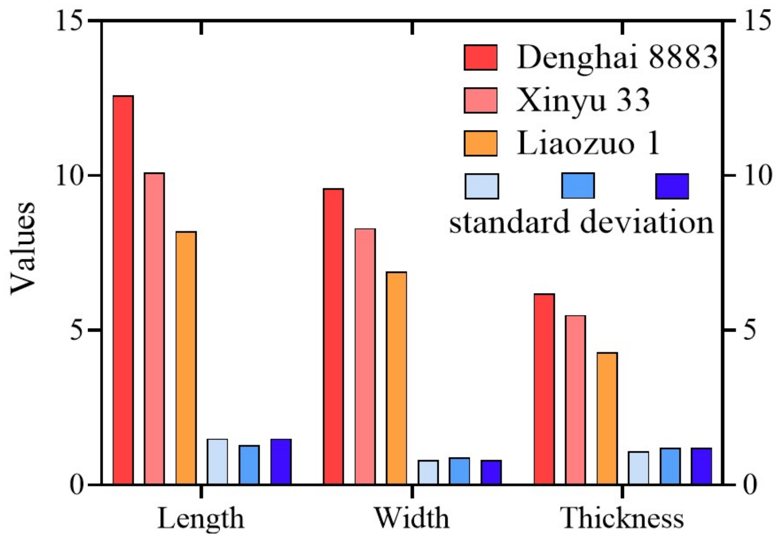

FIGURE 6. Differences in maize seed size.

Analysis of the seed-holding process

In the seed-holding process, the clamping force of the seed-picking block on the seed is mainly provided by the spring force of the torsion spring, the size of which directly affects the operating effect. Too little spring force results in insufficient clamping of the seed, causing the seed to fall off and increasing the rate of missed seeding; too much spring force causes damage to the seed, which affects the germination rate and accelerates the wear of the seed spacer steel ring (Fu et al., 2011). The force analysis of the seed collection block during seed holding is shown in Figure 7.

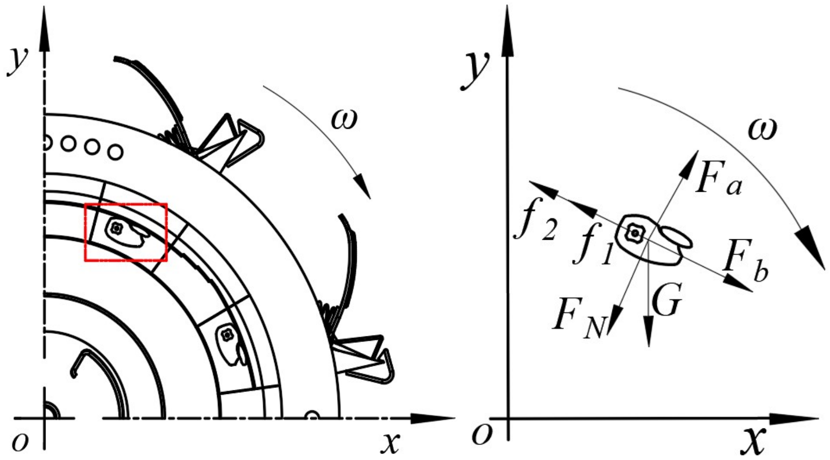

FIGURE 7. Force analysis of the seed-holding process.

To make the seed-picking block move smoothly in the process of seed holding, the moment of the seed-picking block at the center of rotation should be balanced; therefore,

$$\sum M = 0 \tag{1}$$

$$Gl_1 + F_N l_2 = F_a s_1 + f_1 s_2 + f_2 s_3 \tag{2}$$

Where:

M is the torque at the center of rotation of the seed-picking block and F_b is the support force of the abduction arm axis on the seed-picking block. To reduce the rigid impact on the seed, the block is made of resin, so the effect of the gravity of the seed-picking block on M can be ignored, and the above equation can be written as

$$F_N = \frac{F_a s_1 + f_1 s_2 + f_2 s_3}{l_2} \tag{3}$$

in which:

F_N - clamp-holding force of the seed-picking block, N;

F_a - force of the torsion spring, N;

f_1 - friction of the seed spacer steel ring on the seed-picking block, N;

f_2 - friction of the seed grain on the seed-picking block, N;

s_1 - length of the torsion spring's force arm, mm;

s_2 - distance of the seed-picking block rotary center and seed spacer steel ring, mm;

s_3 - radial distance of the seed grain surface and rotary center, mm,

l_2 - normal distance of the seed grain surface and rotary center, mm.

Equation (3) indicates that the clamp-holding force of the seed-picking block on the seed is influenced by the spring force of the torsion spring, the size of the seed-picking block, and the size of the seed. The force analysis of the seed-picking block during seed holding is shown in Figure 8.

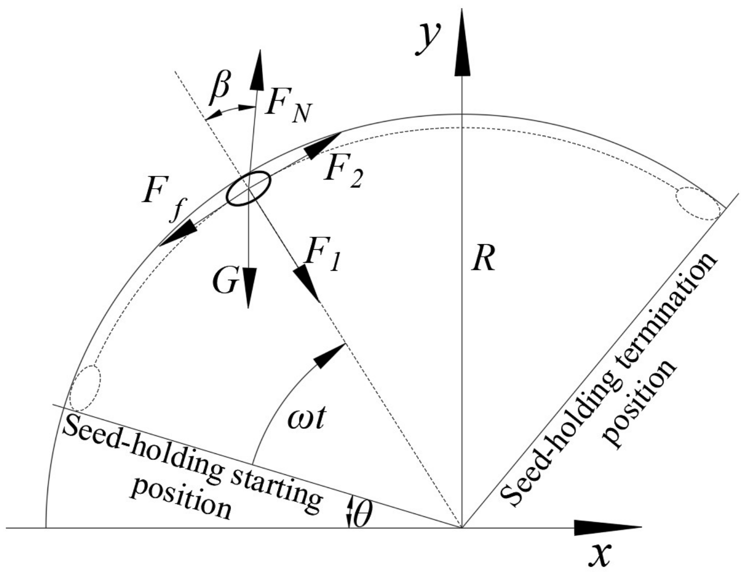

FIGURE 8. Force analysis of maize seed.

Decomposition of the radial force gives:

$$F_1 + G\sin\left(\theta+\omega t\right) - F_N\cos\beta = m\omega^2 R \quad (4)$$

$$F_N = \frac{F_1 + G\sin\left(\theta+\omega t\right) - m\omega^2 R}{\cos\beta} \quad (5)$$

Decomposition of the tangential force gives:

$$F_2 + F_N\sin\beta = \mu F_1 + G\cos\left(\theta+\omega t\right) \quad (6)$$

$$F_1 = \frac{F_2 + F_N\sin\beta - G\cos\left(\theta+\omega t\right)}{\mu} \quad (7)$$

Bringing [eq. (7)] into [eq. (6)] gives:

$$F_N = \frac{F_2 - G\cos\left(\theta+\omega t\right) + \mu G\sin\left(\theta+\omega t\right) - \mu m\omega^2 R}{\mu\cos\beta - \sin\beta} \quad (8)$$

The second-order derivative of ω at both ends gives:

$$\frac{d^2F_N}{d\omega^2} = \frac{gt^2\cos\left(\theta+\omega t\right) - \mu gt^2\sin\left(\theta+\omega t\right) - 2\mu R}{\mu\cos\beta - \sin\beta} \quad (9)$$

In which:

F_1 - support force of the seed spacer steel ring on the seed, N;

F_N - clamping force of the seed-picking block on the seed, N;

m - weight of the seed, kg;

ω - rotational speed of the seed-metering device, rad/s;

R - radius of the seed's rotational movement, mm;

θ - starting angle of the seed-holding area, (°);

t - duration of the seed-holding movement, s;

μ - friction factor between the seed and the seed spacer steel ring,

β - angle of the normal direction of the clamping force, (°).

The value of β is related to the size of the seed, and β takes values from π/9 to 2π/9. From the literature (Chen, 2019), the friction factor between the seed and the seed spacer steel ring can be taken as 0.3. When the value of ($\theta+\omega t$) is less than 7/18π, the second-order derivative is less than zero, and the function curve of F_N is convex. With increasing speed, the clamp-holding force first increases and then decreases. When the value of ($\theta+\omega t$) is greater than 7/18π, the second-order derivative is greater than zero, and the F_N function curve is concave, with the clamp-holding force decreasing and then increasing as the speed increases. To prevent damage to the maize kernels during seed holding, the clamp-holding force F_N should satisfy:

$$F_N\cos\beta < F_{c\min} \quad (10)$$

Where:

F_c is the ultimate compressive load on the maize grain in the thickness direction. From the literature (Zhang et al., 2021b), Fc can range from 80.38 N to 338.72 N, and insertion into [eq. (10)] indicates that F_N can take the maximum value of 82.9 N.

Equations (3) and (9) indicate that the seed-holding performance of the seed-picking block is related to the torsion spring force, the rotational speed of the seed-metering device, and other factors. Selecting the optimum combination of parameters can effectively improve the operational performance of the precision maize-seed-metering device.

Analysis of the seed-clearing process

To improve the seed-picking effect of the seed-filling area, a larger seed-holding section and a longer seed-guiding section are chosen for the seed-picking block. To enhance the seed-picking effect, the seed-picking block is designed to be larger. Because of the large size difference between maize kernels, there is a possibility of holding two seeds laterally, resulting in multiple seeding. To reduce the multiple seeding rate and improve the seed discharge performance, a three-stage stepped seed-clearing structure is designed on the inner wall of the seed spacer steel ring. The seed-clearing area is positioned 45° above the seed-metering device at an angle, as shown in Figure 9.

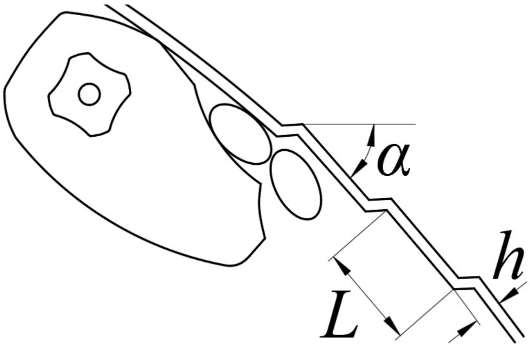

(a) Diagram of the seed-clearing process

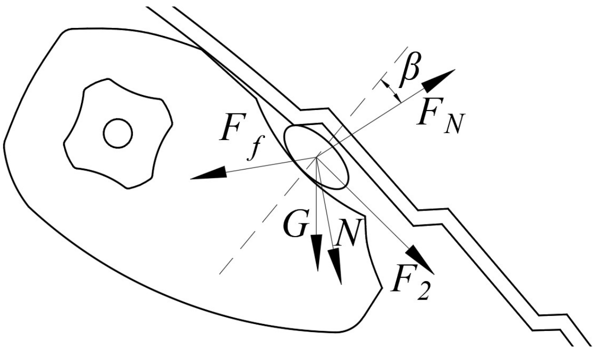

(b) Force analysis of the seed-clearing process

FIGURE 9. Analysis of the seed-clearing process.

The smaller seeds cannot be clamped down when the seed-picking block pushes two seeds with a significant size difference. In this case, the seeds automatically fall back to the seed-filling area during the pushing process. As shown in Figure 9(a), when the seed-picking block enters the seed-clearing area with two seeds of similar size, the force balance of the seed at the front end is disrupted under the seed-clearing ladder, and the seed falls back to the seed-filling area by gravity. The structural dimensions of the seed-clearing area are designed according to the shape parameters of the seed-picking block and the size of the maize seed, mainly including the length of the seed-clearing section (noted as L), the height of the step (noted as h), and the inclination angle of the slope (noted as α). The design should follow:

$$\begin{cases} 1.5l \le L \le 2l \\ 0.3b \le h \le b \end{cases} \tag{11}$$

in which:

l - length of the maize kernel, mm,

b - thickness of the kernel, mm.

By combining the parameters of the seed-picking block with the previously measured maize seed size, L is set to 13 mm and h to 2 mm. As shown in Figure 9(b), in the seed-clearing area, the remaining seed that need to be clamped are all in a nonequilibrium state. To maintain clamping, the force at the moment of clamping on the inclined plane should meet:

$$\begin{cases} F_f \sin\alpha + G\cos\dfrac{\pi}{4} + N\cos\alpha \le F_N \cos\beta \\ F_N \sin\beta + N\sin\alpha + F_2 + G\sin\dfrac{\pi}{4} \le F_f \cos\alpha \end{cases} \tag{12}$$

Introducing the trigonometric auxiliary formula into the above equation gives:

$$\begin{cases} \alpha \le \arcsin\dfrac{F_N\cos\beta - G\cos\dfrac{\pi}{4}}{N\sqrt{\mu^2+1}} - \arctan\dfrac{1}{\mu} \\ \alpha \le \arcsin\dfrac{\mu}{\sqrt{\mu^2+1}} - \arcsin\dfrac{F_N\sin\beta + F_2 + G\sin\dfrac{\pi}{4}}{N\sqrt{\mu^2+1}} \end{cases} \tag{13}$$

Usually, the rotational speed of the seed-metering device (noted as ω) has a value of π/3 rad/s to π/2 rad/s. Considering the overall structure of the seed-metering device and the agronomic requirements of maize sowing, the value of the radius of the rotational movement of the clamped seeds is 135 mm. The weight of the maize kernel (*m*) and gravity (*G*) can be deduced from the maize thousand kernel weight, and the friction coefficient (μ) is constant. The radial clamping angle of the clamping force F_N (β) has a value of π/9 to 2π/9. Considering the location of the clearing area, the value of ($\theta+\omega t$) is set at 135°, and the value of α is set at 45° to reduce the rigid impact of the seed-clearing process on the seed.

Analysis of the seed-dropping process

At the end of the seed-cleaning process, the seed-picking block pushes the single maize seed into the seed-dropping area for the first seed-dropping process. The height of the seed feeding opening on the seed spacer steel ring directly affects the quality of the seed drop. Too low a height causes the seed in the seed-filling area to enter the drop and increases the multiple seeding rate; too high a height increases the throwing force required to deliver the seed, resulting in a higher rate of missed seeds. Combined with the throwing motion curve and the position of the seed population in the seed-metering device, the seed throwing mouth is placed at the horizontal line of the center of the seed-metering device. The first seed-dropping process can be approximated as a parabolic motion, as shown in Figure 10.

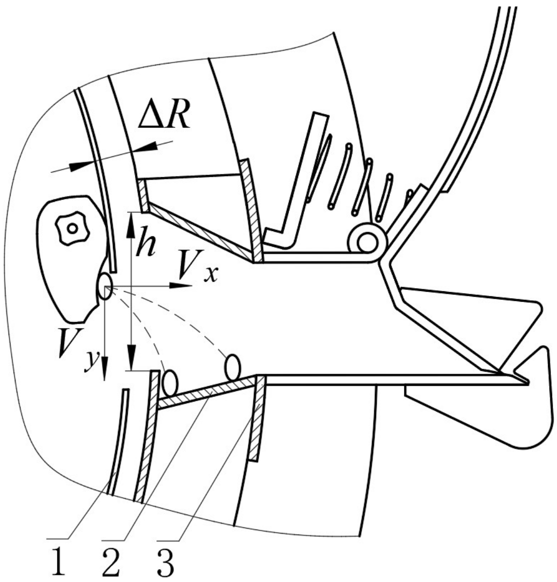

1. seed spacer steel ring 2. Seed-guiding funnel 3. Duckbill base plate

FIGURE 10. Diagram of the first seed-dropping process.

The height of the seed-guiding funnel opening (noted as *h*) is 30 mm, and a baffle is added to the bottom of the funnel opening to prevent the seed from flowing backward. During the throwing process, the initial velocity of the horizontal movement of the seed can be calculated as:

$$V_x = \sqrt{\frac{2F_N l_1}{m}} \tag{14}$$

In which:

F_N - clamp-holding force of the seed-picking block, N;

l_1 - length of the working displacement of F_N during the seed-picking process, calculated as:

$$l_1 = L_3 \sin\beta \tag{15}$$

In which:

β - angle of the normal direction of the clamping force (°)

L_3 - length of the working section on the seed-picking block, which is set at 8 mm.

Then, the movement time of the seed during throwing can be calculated as follows:

$$t = \frac{\Delta R}{V_x} = \frac{\Delta R\sqrt{m}}{\sqrt{2F_N L_{AB}\sin\beta}} \tag{16}$$

Where:

ΔR is the length of the gap between the seed spacer steel ring and the funnel mouth; the value is 7 mm. Then, the vertical displacement of the seed during the throwing process L_y can be calculated as follows:

$$L_y = \frac{1}{2}gt^2 \tag{17}$$

To enable the seed to be thrown smoothly into the seed guide funnel and to take into account the effect of vibration on the seed-dropping process during actual operation, the throwing process, L_y, during the throwing process should meet:

$$L_y < \frac{1}{2}h \tag{18}$$

Substituting [eq. (16)] for [eq. (17)] gives:

$$F_N > \frac{mg\Delta R}{2L_{AB}h\sin\beta} \tag{19}$$

Substituting each value gives a minimum value of F_N of 0.12 N, and the torsion spring's wire diameter can be calculated as:

$$F_N = \frac{9.8Ed^4\theta}{1167D_m\pi NR} \tag{20}$$

In which:

E - elastic modulus of the steel wire, taken as 19400 for stainless steel wire;

θ - angle of torsion spring turning, (°);

d - diameter of the torsion spring wire, mm;

D_m - pitch diameter of the torsion spring, mm;

N - number of torsion spring turns,

R - length of the load force arm, mm.

Through comprehensive analysis, the value of (D_m) is set at 10 mm, the value of the number of turns (N) is 8, the value of (θ) is π/6, and the length of the force arm (R) is 13 mm. Therefore, the minimum value of the torsion spring wire diameter (d) is 1.46 mm when brought into [eq. (19)].

Bench testing

Test conditions

Based on the theoretical analysis, a prototype of a clamp-holding precision maize-seed-metering device was made, and a bench test is carried out. The test seeds are selected from the Xinyu 33 maize kernels, which are widely grown in China. The seed-metering device is mounted on the seed-metering device's test stand for testing, as shown in Figure 11.

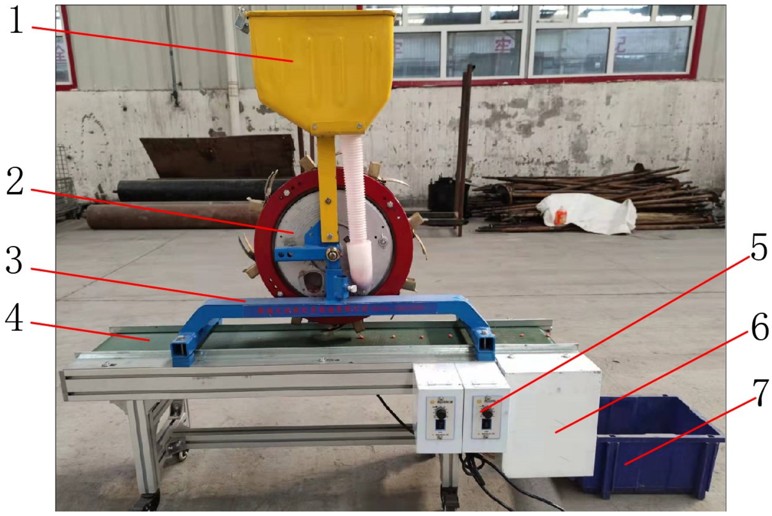

1. Seed box 2. Seed-metering device 3. Support bracket 4. Conveyor belts 5. Console 6. Voltage stabilizer 7. Seed collection box

FIGURE 11. Test stand of the seed-metering device.

Test indicators

To check the quality of the seed dispenser operation, the qualified rate, multiple seeding rate, and missed seeding rate are selected as evaluation indicators. Where the qualified rate is the single seed rate of the seed-metering device. The values of each evaluation indicator are calculated according to the following formula:

$$\theta = \frac{g}{G} \times 100\% \tag{21}$$

In which:

θ - qualified rate, multiple seeding rate, and missed seeding rate, %;

g - number of single seeding holes, multiple seeding holes, and missed seeding holes,

G - total number of holes measured.

Experimental factors

According to the theoretical analysis and preliminary experiments, the torsion spring's wire diameter (A), the seed-metering device's rotational speed (B), and the limit guide plate's installation radius (C) are selected as experimental factors. The preset values of each factor are shown in Table 1.

TABLE 1. Experimental factors and levels.

Level	A(mm)	B(mm)	C(mm)
1	1.5	20	90
2	1.6	25	93
3	1.7	30	96

Figure 12 shows the variation values of spring force with torsion angle for torsion springs of different filament diameters. The larger the wire diameter of the torsion spring is, the greater the rate of change in the torsion spring force, which leads to a large impact of the seed picker on the seed. To prevent damage to the seed, the rate of change in the torsion spring force should be small, so torsion spring wire diameters of 1.5 mm, 1.6 mm, and 1.7 mm are selected.

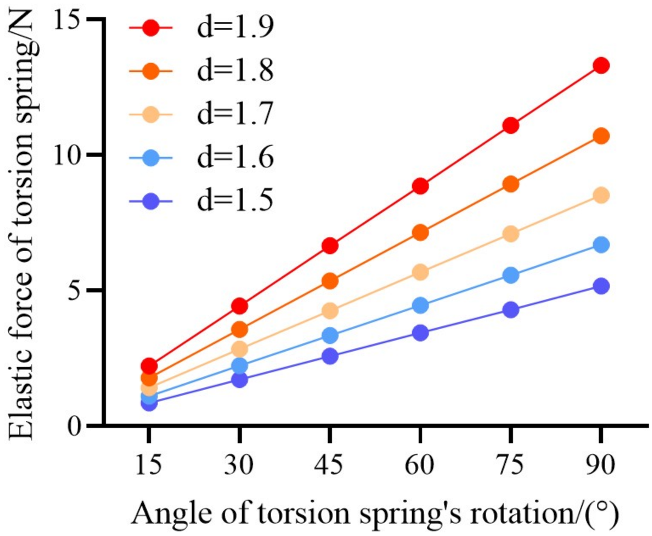

FIGURE 12. Elastic force change rate of the torsion spring.

RESULTS AND DISCUSSION

Nine groups of tests were conducted each time, and 250 holes were taken from each group to record the data. The test was repeated three times to obtain the average value. Equation (21) was used to calculate the qualified rate, multiple seeding rate, and missed seeding rate. To determine the effect of the error on the test results, a blank column was added to the orthogonal test design table denoted as *D*. The orthogonal test table and the test results are shown in Table 2.

TABLE 2. Test results.

No.		Experimental factors				Qualified rate /%	Multiple seeding rate /%	Missed seeding rate /%
		A	*B*	*C*	*D*			
1		1	1	1	1	89.32	3.84	6.84
2		1	2	2	2	95.54	2.98	1.48
3		1	3	3	3	86.15	6.72	7.13
4		2	1	2	3	95.86	2.78	1.36
5		2	2	3	1	94.21	4.77	1.02
6		2	3	1	2	87.52	4.72	7.76
7		3	1	3	2	89.75	6.98	3.27
8		3	2	1	3	91.73	3.95	4.32
9		3	3	2	1	90.05	5.72	4.23
Qualified rate	k_1	90.34	91.64	89.52	91.19			
	k_2	92.53	93.83	93.82	90.94			
	k_3	90.51	87.91	90.04	91.25			
	R_1	2.19	5.92	4.29	0.31			
	Factor priorities:*B*>*C*>*A*							
	Better combination:$A_2B_2C_2$							
Multiple seeding rate	k_1	4.51	4.53	4.17	4.78			
	k_2	4.09	3.9	3.83	4.89			
	k_3	5.55	5.72	6.16	4.48			
	R_2	1.46	1.82	2.33	0.41			
	Factor priorities:*C*>*B*>*A*							
	Better combination:$A_2B_2C_2$							
Missed seeding rate	k_1	5.15	3.82	6.31	4.03			
	k_2	3.38	2.27	2.36	4.17			
	k_3	3.94	6.37	3.81	4.27			
	R_3	1.77	4.10	3.95	0.24			
	Factor priorities:*B*>*C*>*A*							
	Better combination:$A_2B_2C_2$							

The data in Table 2 were counted and plotted in Figure 13, from which it can be seen that the qualified rate in each group of trials was greater than 85%, the multiple seeding rate was less than 10%, and the missed seeding rate was less than 8%, meeting industry standards.

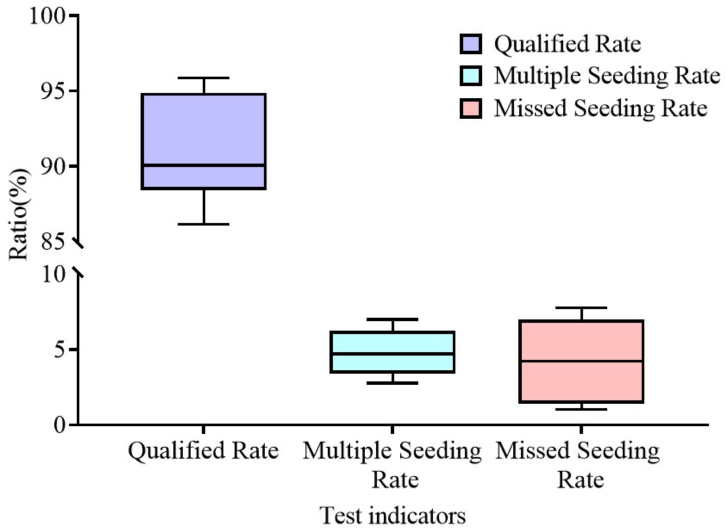

FIGURE 13. Statistical graph of results.

As seen from Table 2, the primary and secondary order of influence of the factors on the qualified rate and the missed seeding rate is $B>C>A$; the primary and secondary order of influence of the factors on the multiple seeding rate is $C>B>A$.

$A_2B_2C_2$ is the preferred solution for increasing the qualified rate, i.e., a torsion spring wire diameter of 1.6 mm, a seed-metering device rotational speed of 25 r/min, and a limit guide plate installation radius of 93 mm. The pattern of influence of the level of each factor on the performance indicators of the seed-metering device is shown in Figure 14.

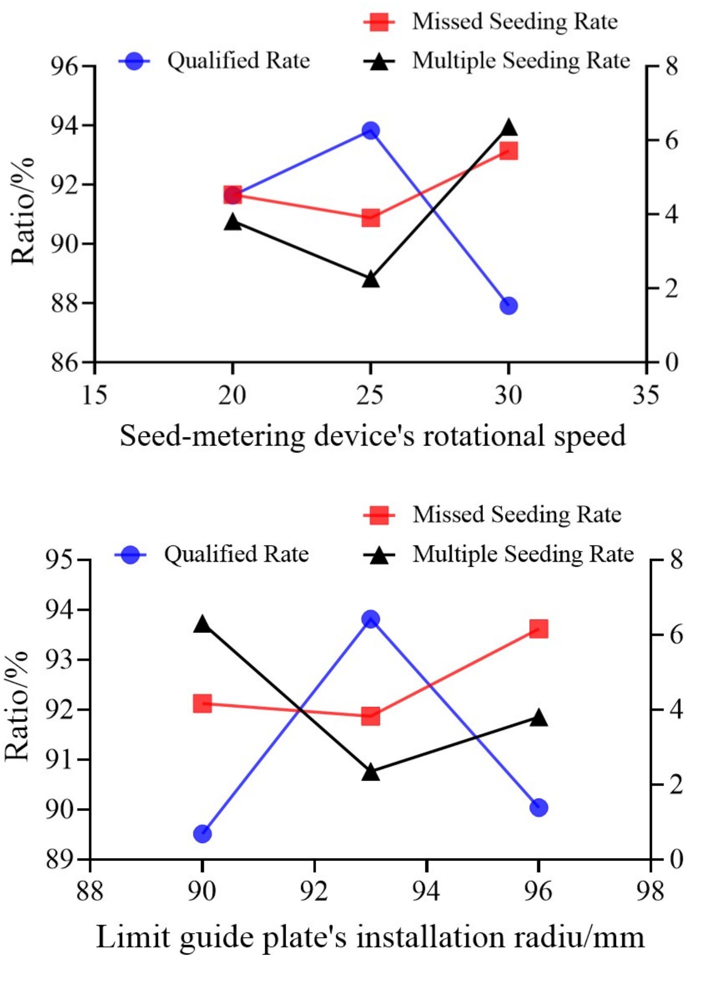

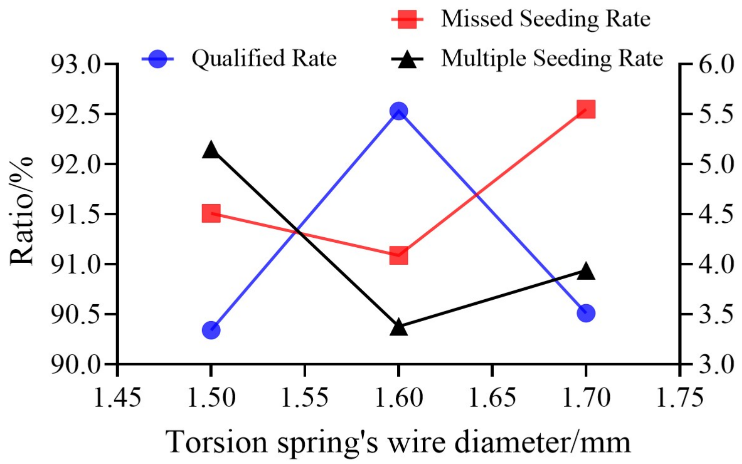

FIGURE 14. Influence of factors on performance indicators.

Field validation test

To verify the working performance of the seed-metering device in the field, field validation trials were carried out, as shown in Figure 15. The firmness of the land was 458 kPa, the water content was 9.7%, the surface was flat and free from obstacles, and the quality of the land met the agronomic requirements for maize sowing.

FIGURE 15. Field validation test.

The tractor was driven at a speed of approximately 2.0 km/h. Each measurement was carried out 20 m after sowing, 250 holes were measured continuously, the number of single seeding holes, multiple seeding holes, and missed seeding holes were counted, and the average value was obtained by repeating the test three times. The results of the experiment are shown in Table 3 and Figure 16. With an improved combination of parameters, the qualified rate was 94.21%, the multiple seeding rate was 3.52%, and the missed seeding rate was 2.27%, meeting the agronomic requirements for maize sowing.

TABLE 3. Experimental verification results.

No.	Qualified rate	Multiple seeding rate	Missed seeding rate
1	94.36	3.19	2.18
2	93.81	3.51	2.24
3	94.46	3.86	2.39
Average	94.21	3.52	2.27

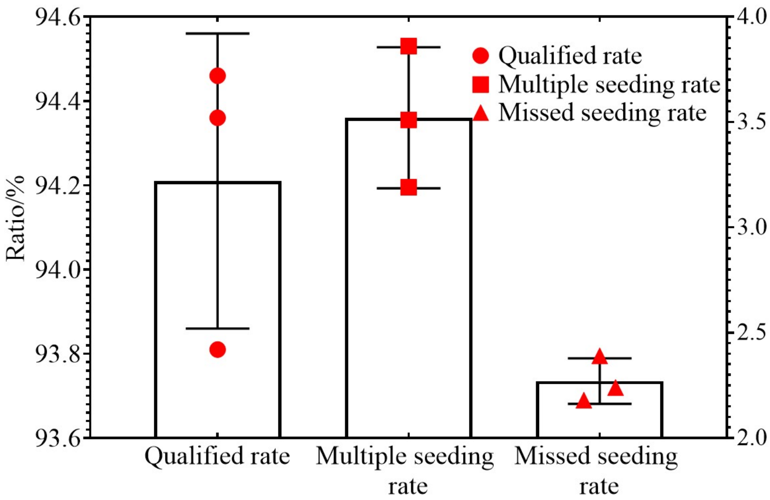

FIGURE 16. Experiment verification results.

CONCLUSIONS

Compared with the existing research, the operational performance of the seed-metering device designed in this paper is more stable, and it is easy to repair and maintain. In view of the above advantages, this paper is centered on the following elements:

A clamp-holding precision maize-seed-metering device was designed, and its structure and working principle were introduced. The structural parameters of the critical components were determined by analyzing the mechanics of the seed-picking blocks and the movement of the seeds in different operating areas.

The limit guide plate mechanism of the force locking cam contour was designed. By controlling the opening and closing of the seed-picking block through a simple harmonic motion curve, the rigid impact of the seed-picking block on the seed is reduced, and the operation is smooth and reliable.

The prototype of a clamp-holding precision seed-metering device for maize was trial produced. A bench-top orthogonal test was carried out with the torsion spring's wire diameter, the seed-metering device's rotational speed, and the installation radius of the limit guide plate as test factors and the qualified rate, multiple seeding rate, and missed seeding rate as test indicators to determine the optimal combination of parameters: a torsion spring wire diameter of 1.6 mm, a seed-metering device rotational speed of 25 r/min and a limit guide plate installation radius of 93 mm. Field validation trials with the optimum combination of parameters yielded a qualified rate of 94.21%, a multiple seeding rate of 3.52%, and a missed seeding rate of 2.27%, meeting the agronomic requirements for maize sowing.

ACKNOWLEDGMENTS

This work was supported by Xinjiang agricultural machinery R & D, manufacturing, promotion and application of integrated projects (No. YTHSD2022-02); Major Science and Technology Special Projects in the Autonomous Region (No. 2022A02003-3) and the regional Collaborative Innovation Special Project (Science and Technology Assistance Program) in the Autonomous Region, China (No. 2021E02055).

REFERENCES

Astanakulov K, Baimakhanov K, Alpamyssova G, Babojanov A (2021) Development of a pneumatic drum-type seeding apparatus for two-row seeding soybean and mung bean. IOP Conference Series: Earth and Environmental Science 839(5):052062.

Balappa BU, Lokesh AC, Babu NCM (2021) Development of semi-automated sowing machine for multiple crops. Materials Today: Proceedings 42:1317-1320.

Chen ZR (2019) An approach to and validation of maize-seed-assembly modelling based on the discrete element method. China, Jilin University.

Fu W, Li SF, Sun JY, Yang HY, Kan Z (2011) Forced clamping type corn precision seed discharger. Transactions of the Chinese Society of Agricultural Engineering 27(12):38-42.

Geng DY, Li YH, Meng PX, Du RC, Meng FH (2016) Design and test of a telescopic finger clamp seed rower for maize. Transactions of the Chinese Societyof Agricultural Machinery 47(5):38-45.

Li CH, Xia JM, He B (2004) Analysis and experiment of seed metering procedure in scoop metering device with declined disc. Transactions of the Chinese Society of Agricultural Machinery (03):68-71.

Li HC, Gao F, Zhao Z, Liu W (2014) Analysis about dual dynamic mechanism of popularizing conservation tillage technology. Journal of Chinese Agricultural Mechanization 35(2):12-16+56.

Li YH, Yang L, Zhang DX, Cui T, Zhang KL, Xie CJ, Yang RM (2020) Analysis and test of linear seeding process of maize high speed precision metering device with air suction. Transactions of the Chinese Society of Agricultural Engineering 36(9):26-35.

Liao YT, Li CL, Liao QX, Wang L (2020) Research progress of seed guiding technology and device of planter. Transactions of the Chinese Society of Agricultural Machinery 51(12):1-14.

Liu J, Cui T, Zhang DX, Yang L, Gao NN, Wang B (2010) Effect of seed grading treatment on the sowing effect of pneumatic precision seeders. Transactions of the Chinese Society of Agricultural Engineering 26(9):109-113.

Pareek CM, Tewari VK, Machavaram R, Nare B (2021) Optimizing the seed-cell filling performance of an inclined plate seed metering device using integrated ANN-PSO approach. Artificial Intelligence in Agriculture 5:1-12.

Singh I, Gautam A, Dixit AK, Manes GS, Singh A (2020) Development and evaluation of inclined plate metering mechanism for the sowing of maize (Zea mays L) seed. Current Journal of Applied Science and Technology 39(13):118-128.

Singh UV, Moses SC (2021) Development and testing of manually operated single row planter for groundnut seeds. International Journal of Farm Sciences 11(1, 2):93-101.

Wang B, Na Y, Liu J, Wang Z (2022) Design and evaluation of vacuum central drum seed metering device. Applied Sciences 12(4):2159.

Wang Q, Zhu LT, Li MW, Huang DY, Jia HL, Zhuang J (2019a) Vibration characteristics of corn no-tillage finger-type precision planter and its effect on seeding performance. Transactions of the Chinese Society of Agricultural Engineering 35(9):9-18.

Wang YC, Gao YP, Tai WS, Li BQ, Zhang W, Han X (2019b) Design and experiment of clamping maize precision seed-metering device. Transactions of the Chinese Society of Agricultural Machinery 50(9):40-46.

Yang L, Yan BX, Zhang DX, Zhang TL, Wang YX, Cui T (2016) Research progress of precision seeding technology for corn. Transactions of the Chinese Society of Agricultural Machinery 47(11):38-48.

Yuan YW, Bai HJ, Fang XF, Wang DC, Zhou LM, Niu K (2018) Research progress on maize seeding and its measurement and control technology. Transactions of the Chinese Society of Agricultural Machinery 49(9):1-18.

Zhang CY, Kang JM, Peng QJ, Zhang NN, Wang XY, Jian SC (2021a) Design and test of secondary seed feeding mechanism of air-suction roller dibbler for cotton. Transactions of the Chinese Society of Agricultural Machinery 52(6):106-116.

Zhang T, Liang T, Li P, Liu KS, Zhang XF, Tang XL, Li Y (2021b) Study on basic physical properties and mechanical damage rule of maize seeds. Seed 40(11):46-53.